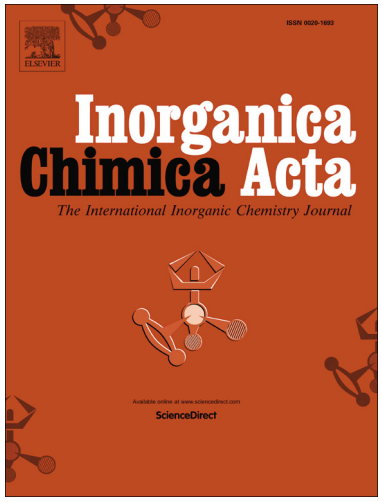

Research paper

Synthesis, crystal structure and cytotoxicity assays of a copper(II) nitrate complex with a tridentate ONO acylhydrazone ligand. Spectroscopic and theoretical studies of the complex and its ligand

Y. Burgos-Lopez, J. Del Plá, L.M. Balsa, I.E. León, G.A. Echeverría, O.E. Piro, J. García-Tojal, R. Pis-Diez, A.C. González-Baró, B.S. Parajón-Costa

PII: S0020-1693(18)31251-9
DOI: https://doi.org/10.1016/j.ica.2018.11.039
Reference: ICA 18654

To appear in: *Inorganica Chimica Acta*

Received Date: 19 August 2018
Revised Date: 11 October 2018
Accepted Date: 24 November 2018

Please cite this article as: Y. Burgos-Lopez, J. Del Plá, L.M. Balsa, I.E. León, G.A. Echeverría, O.E. Piro, J. García-Tojal, R. Pis-Diez, A.C. González-Baró, B.S. Parajón-Costa, Synthesis, crystal structure and cytotoxicity assays of a copper(II) nitrate complex with a tridentate ONO acylhydrazone ligand. Spectroscopic and theoretical studies of the complex and its ligand, *Inorganica Chimica Acta* (2018), doi: https://doi.org/10.1016/j.ica.2018.11.039

Synthesis, crystal structure and cytotoxicity assays of a copper(II) nitrate complex with a tridentate ONO acylhydrazone ligand. Spectroscopic and theoretical studies of the complex and its ligand

Y. Burgos-Lopez[a], J. Del Plá[a], L.M. Balsa [a], I.E. León[a], G.A. Echeverría[b], O.E. Piro[b], J. García-Tojal[c], R. Pis-Diez[a], A.C. González-Baró[a] and B.S. Parajón-Costa[a*]

[a] CEQUINOR (CONICET, CCT-La Plata, UNLP), Bvd. 120 N°1465, B1900AVV- La Plata, Argentina. [a*] beatrizp @ química.unlp.edu.ar

[b] Departamento de Física, Facultad de Ciencias Exactas, Universidad Nacional de La Plata and IFLP (CONICET, CCT-La Plata), C.C. 67, B1900AVV - La Plata, Argentina

[c] Departamento de Química, Universidad de Burgos, Pza. Misael Bañuelos s/n, E-09001 Burgos, España.

Abstract

The new copper complex, $[Cu(HL)(OH_2)_2](NO_3)$, including the tridentate N-acyhydrazone derived from 4-hydroxy-benzohydrazide and 2-hydroxy-3-methoxybenzaldehyde, (H_2L), has been synthesized and characterized in the solid state and in solution by spectroscopic (FTIR, Ra, UV-vis, EPR) methods. The results were compared with those obtained for the hydrazone ligand and complemented with computational methods based on DFT. The crystal structure of the complex has been determined by X-ray diffraction. It crystallizes in the triclinic $P\bar{1}$ space group with Z = 2. The Cu(II) ion is in a distorted square pyramidal environment, coordinated to a planar HL^- anion acting as a tridentate ligand. The 5-fold coordination is completed with two water molecules. It is arranged in the lattice as H-bonded ribbon-like polymers that extends along the [121] crystal direction. The cytotoxicity of the complex together with that of the H_2L ligand and the copper ion were evaluated *in vitro* against five different human cancer cell lines namely A549 (lung), MG-63 (bone), MCF-7 and MDA-MB.231 (breast) and Jurkat (leukemia). The copper complex inhibits the cell viability in a dose dependent manner with a greater potency than the H_2L ligand and the free copper ion displaying even higher antitumor activity than the well-known anticancer metallodrug cisplatin.

Keywords: Cu(II)-complex; Hydrazones; Spectroscopy; Crystal structure; DFT calculations, Anticancer activity.

1. Introduction

Hydrazones and aroyl /acyl hydrazones (RC(H)=N-NR^{1}R^2) are an interesting family of organic compounds because of their recognized physiological and biological activities as well as for their numerous chemical applications. Their therapeutic properties make them attractive materials for the development of new drugs of relevance in medicinal chemistry field [1-3].They are also becoming increasingly important in coordination chemistry [4] and in the design of new sensors and compounds of interest in the field of no-linear optics and supramolecular chemistry [5]. They have been employed as molecular photoswitches [6], as analytical reagents for the determination of metal ions [7], as catalysts and as precursors or intermediates for the synthesis of many organic compounds [8]. Their structural characteristic determines their physicochemical properties and consequently their wide spectrum of applications. The–(H)C=N-N< skeleton contains an imine carbon that has both electrophilic and nucleophilic character and two nucleophilic nitrogen atoms. The azomethine sp^2-nitrogen –N=CH- has been considered of significance in biological interactions whereas the amino sp^3-nitrogen is more reactive as it has a lone pair of electrons and, in most cases, an acidic proton [5]. N-acylhydrazones, which are obtained by condensation reaction of hydrazides or substituted hydrazides with aldehydes or ketones, contain a carbonyl group (-(H)C=N-N(H)C=O) that increases the electron delocalization and denticity of the compound when acts as a ligand.

On the other hand, the possibility of a configurational change around the C=N double bond contributes to the formation of two geometrical isomers, either E or Z, being generally the E isomer thermodynamically more stable [5,9]. Also, the presence of the amide –(H)N-C=O- functionality enables the existence of tautomeric equilibrium between the keto-amine (amido) and the enol-imino (iminol) forms (*Scheme 1*). However, the equilibrium is often observed in solution whereas in the solid state these hydrazones are usually obtained in the amido tautomeric form. (RC(H)=N-NR^{1}R^2).

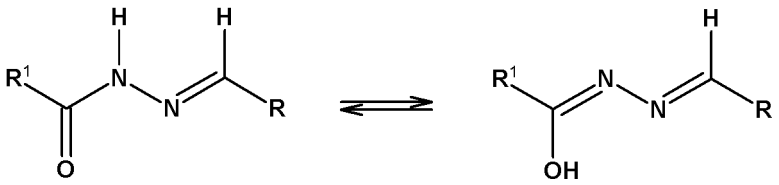

keto-amine (amido) enol-imine (iminol)

Scheme 1. Proposed tautomeric forms of N-acyl hydrazones

Thus, the structural diversity and flexibility of these compounds allow them to interact with metal ions through different coordination modes. Their biological and physiological properties are

related with their capacity to form stable chelates with metal ions that play an essential role as catalysts of many biochemical processes [10]. Currently, the design and synthesis of new compounds containing N-acylhydrazones coordinated to transition metal ions in different oxidation states is considered a promising approach in the discovery of new drugs for the clinical treatment of numerous diseases [9,10].

Among the transition metals, copper is an essential trace element for all living organisms and one of the most prevalent in the human body. It plays a fundamental role in cell physiology as essential component of many metalloproteins and enzymes, being involved as a catalytic cofactor in various metabolic oxidation/reduction processes [11,12]. However, it can be also toxic, and some diseases are related with an imbalance between the intra and extracellular contents of this element in the body [11-13]. On the other hand, it is well known that several families of copper compounds are employed for the clinical treatment of many diseases. In particular, since the approval of cisplatin and platinum-based drugs as effective chemotherapeutics, several research groups have developed and evaluated many copper complexes as a new generation of non-platinum antitumor agents. It is proposed that they could overcome some of the disadvantages associated with cisplatin therapy and that their "*in vitro*" and/or "*in vivo*" demonstrated cytotoxicity could be understood considering a different mechanism of action, bio-distribution and toxicity from those known for platinum-based drugs [13,14]. Specifically, in the last years the therapeutic potentiality of copper hydrazones as antitumoral, [13-17], antioxidant [16,18], antimicrobial and antibacterial agents[9,19,20], among others properties, have been determined.

Recently, our group has reported a structural, spectroscopic and theoretical study of the N-acylhydrazone obtained as a condensation product of isoniazid and o-vanillin (INHOVA) [21] and of its oxidovanadium(V) ester-like complex of formula [VO(INHOVA)EtO(H_2O)]Cl.H_2O [22]. In this compound, the hydrazone coordinates to the vanadium centre as a monoanion, due to the protonation of the pyridinic nitrogen, through the ONO chelating system. Furthermore, studies of cytotoxicity show that the activity of the complex against the chronic myelogenous leukemia K562 cell line is slightly higher than that of the ligand [22].

As part of the project on hydrazones derived from hydroxy aldehydes and aromatic hydrazides and their coordination compounds, herein we report the synthesis and physicochemical characterization of the new nitrate copper(II) complex, [Cu(HL)(OH_2)$_2$] (NO_3), (complex (I) from now on) where H_2L is the neutral stable N-acylhydrazone ligand obtained by condensation reaction of 4-hydroxy-benzohydrazide (4-HBH) with 2-hydroxy-3-methoxybenzaldehyde, (*o*-vanillin: *o*-HVa), according to a previously reported procedure [23], and HL^- is the monodeprotonated anion (see *Scheme 2*).

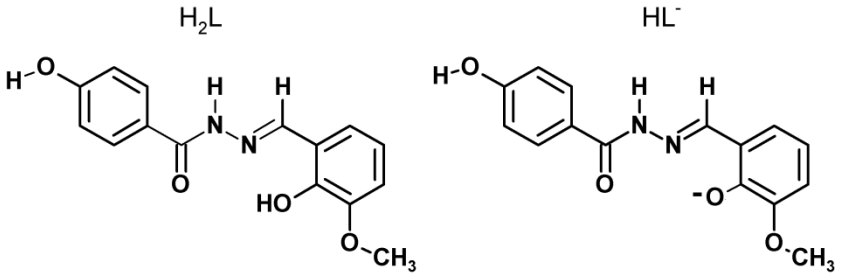

Scheme 2. Schematic representation of 4-hydroxy-N´-[(E)2-hydroxy-3methoxybenzylidene] benzohydrazide (H_2L) and its monoanion (HL^-).

The geometric properties of the complex (1) were determined by X-ray diffraction method and compared with those of the free ligand, whose crystal structure has been already reported [23]. Quantum chemical studies of both compounds were also carried out. The optimized geometry, the harmonic vibrational frequencies and the electronic transitions of both compounds were calculated using methods based on the density functional theory (DFT). The experimental vibrational modes and electronic transitions were assigned with the support of the theoretical results. Further, the "*in vitro"* cytotoxicity of the complex against five cancer cell lines, MG-63 (bone), A549 (lung), Jurkat (leukemia), MCF-7 (breast), MDA-MB-231(breast), was evaluated and compared with those of the free ligand, the copper nitrate salt and the reference anticancer metallodrug cisplatin.

2-Experimental

2.1. Materials and Methods

All starting materials and reagents were of analytical grade. 2-hydroxy-3-methoxybenzaldehyde (Sigma), 4-hydroxybenzhydrazide (Sigma), $Cu(NO_3)_2.2.5H_2O$ (Riedel de Haën), methanol (MeOH, Carlo Erba), absolute ethanol (EtOH, Emsure), 96% ethanol (EtOH, PuroCol) and dimethylsulfoxide (DMSO, Merck) were used as purchased without further purification.

Tissue culture materials were purchased from Corning (Princeton, NJ, USA), Dulbecco's modified Eagle's medium (DMEM) and TrypLE ™ were obtained from Gibco (Gaithersburg, MD, USA), and fetal bovine serum (FBS) was purchased from Internegocios (Argentina). All the cell lines were purchased from ATCC (American Type Culture Collection).

2.2. ***Synthesis of [Cu(HL)(OH$_2$)$_2$](NO$_3$) (1)***

20 mL of 96% ethanol solution of the hydrazone ligand (0.1521g, 0.5 mmol) was drop-wise added under continuous stirring to a 96% ethanolic solution (20 mL) of $Cu(NO_3)_2.2.5H_2O$

(0,1163g, 0.5 mmol). During the ligand addition, the initial blue colour of the copper solution gradually changed to a final dark green colour. The reaction mixture was stirred during 5 hours at 50°C and the resulting bright green solution was then let to stand at room temperature. After approximately one month, green single crystals suitable for X- ray structural analysis were obtained. The complex is stable in air and soluble in DMSO, DMF, EtOH and MeOH. Yield: % 55 (0.1477 g). Mp: 275-277°C. Anal. Calc. for $C_{15}H_{17}CuN_3O_9$: C: 40.32%, H: 3.83%, N: 9.40 %. Found: C: 40.36, H: 3.48, N: 9.24%.

2.3. Physicochemical Methods

Elemental analysis (C, H, N) was performed using a Exceter CE 440 analyzer. Melting points (Mp) were obtained with a Bock Monoscop "M" instrument. FTIR spectra (4000-400 cm^{-1}) were measured with a FTIR Bruker EQUINOX 55 instrument, using the KBr pellet technique. Raman spectra were obtained with a WITEC alpha 300 RA spectrophotometer, using laser excitation wavelength of 532 nm and a 20x and 50x objective lenses for H_2L and complex (1), respectively. Electronic spectra of the ligand and the copper complex were recorded in the 200-800 nm spectral range in freshly prepared solution of DMSO and MeOH with a Shimatzu UV-2006 spectrophotometer, using 10 mm quartz cells. Stability measurements in DMSO were recorded in the same spectral range at room temperature at various interval times, during 72 h.

The X-ray diffraction measurements for complex (1) were performed on an Oxford Xcalibur Gemini, Eos CCD diffractometer with graphite-monochromated MoKα (λ =0.71073 Å) radiation. X-ray diffraction intensities were collected (ω scans with ϑ and κ-offsets), integrated and scaled with CrysAlisPro [24] suite of programs. The unit cell parameters were obtained by least-squares refinement (based on the angular setting for all collected reflections with intensities larger than seven times the standard deviation of measurement errors) using CrysAlisPro. Data were corrected empirically for absorption employing the multi-scan method implemented in CrysAlisPro. The structure was solved by intrinsic phasing with SHELXT of the SHELX package [25] and the molecular model refined by full-matrix least-squares refinement with SHELXL of the same suit of programs. The hydrogen atoms were located in a difference Fourier map phased on the heavier atoms. All but the methyl H-atoms were refined at their found positions with isotropic displacement parameters. The water H-atoms were refined with Ow-H and H…H distances restrained to target values of 0.86(1) and 1.36(1) Å, respectively, and their displacement parameter set equal to 1.5 times the equivalent isotropic displacement parameter of the corresponding oxygen atom. The methyl group was refined with the riding model and the location of their H-atoms optimized by treating them as rigid $–CH_3$ groups allowed to rotate during the refinement around

the O-CH_3 bond such as maximize the sum of the residual electron density at the calculated H-positions. Crystal data and structure refinement results are summarized in Table 1.

Table 1. Crystal data and structure refinement results for complex (1).

Empirical formula	$C_{15}H_{17}CuN_3O_9$
Formula weight	446.86
Temperature	293(2) K
Wavelength	0.71073 Å
Crystal system	Triclinic
Space group	$P\bar{1}$
Unit cell dimensions	a = 6.7948(5) Å
	b = 9.2007(5) Å
	c = 15.622(1) Å
	α = 99.753(5)°
	β = 94.004(6)°
	γ = 109.597(6)°
Volume	898.3(1) $Å^3$
Z, density (calculated)	2, 1.652 Mg/m^3
Absorption coefficient	1.272 mm^{-1}
F(000)	458
Crystal dimensions	0.072, 0.100, 0.155
Crystal color	Green
ϑ-range for data collection	2.977 to 29.070°
Index ranges	$-9 \le h \le 9$, $-11 \le k \le 12$, $-20 \le l \le 19$
Reflections collected	7302
Independent reflections	3872 [R(int) = 0.0316]
Observed reflections [I>2σ(I)]	2784
Completeness to ϑ = 25.242°	99.9 %
Refinement method	Full-matrix least-squares on F^2
Data / restraints / parameters	3872 / 6 / 306
Goodness-of-fit on F^2	1.007
Final R indices [I>2σ(I)]	R1 = 0.0552, wR2 = 0.1281
R indices (all data)	R1 = 0.0814, wR2 = 0.1476
Largest diff. peak and hole	1.335 and -1.091 $e.Å^{-3}$

X-band EPR spectra were acquired on a polycrystalline sample by using a Bruker EMX spectrometer, equipped with a Bruker ER 036TM NMR-teslameter and an Agilent 53150A microwave frequency counter. SimFonia program [26] was used to perform the simulated spectra

and graphics were carried out with Kaleidagraph v3.5 [27]. Experimental details: modulation amplitude 0.1 mT, time constant 40.96 ms, conversion time 327.68 ms, gain $1x10^3$ (short ranges) or $1x10^4$ (long 0 - 700 mT ranges) and power 20 mW. Microwave frequencies: 9.3700 (298 K), and 9.4264 (150 K) (Figure S3 of the electronic supplementary information, ESI), and 9.4243 GHz (Figure 3, see below).

2.4. Computational Details

The conformational space of H_2L was investigated by means of the systematic variation of torsion angles involving the C(O)-N-N=C moiety. In the conformational search, the structure of the ligand taken from reported crystallographic data was also considered [23]. For the copper complex only the experimental structure obtained from X-ray diffraction methods was taken into account for the computational study.

All the geometries were optimized using the Becke's three parameters hybrid density functional [28] with the gradient-corrected correlation functional due to Lee, Yang, and Parr [29] as implemented in version 3.0.3 of the ORCA program [30]. The Def2-TZVP basis set of triple-zeta quality was used for all the atoms [31]. To verify whether the optimized geometries are local minima or saddle points on the potential energy surface of the molecules the eigenvalues of the Hessian matrix of the total energy with respect to the nuclear coordinates were calculated. Those eigenvalues were then transformed to harmonic vibrational frequencies, which were further used to aid in the assignment of the experimental vibrational frequencies. Calculated frequencies were not scaled.

The electronic spectra of the ligand and the complex were calculated using the hybrid PBE0 functional [32] with the aug-cc-pVTZ [33,34] basis set. Solvent effects were included implicitly through the Conductor-like Screening Model (COSMO) [35] as implemented in the ORCA program.

2.5. Biological assays

2.5.1. Preparation of the solutions

Fresh stock solutions of H_2L and compound 1 were prepared in dimethyl sulfoxide (DMSO) at 20 mM and they were diluted with DMEM according to the concentrations indicated in Figure 5. Precautions should be taken with the maximum concentration of DMSO in the well plate. Consequently, it was used 0.5 % as the maximum DMSO concentration in order to avoid toxic effects of this solvent on cells.

2.5.2. Cell line and growth conditions

MG-63 (bone), A549 (lung), MCF-7 (breast), Jurkat (leukemia) cancer cells were grown in DMEM containing 10 % FBS, 100 U/mL penicillin, and 100 µg/mL streptomycin at 37° C in a 5 % CO_2 atmosphere whilst MDA-MB-231 (breast) were grown in F12-DMEM. Cells were seeded in a 75-cm^2 flask, and when 70–80 % of confluence was reached, cells were subcultured using 1 mL of TrypLE ™ per 25-cm^2 flask. For experiments, cells were grown in multiwell plates. When cells reached the desired confluence, the monolayers were washed with PBS and were incubated under different conditions according to the experiments.

2.5.3. Cell viability study: 3-(4,5-Dimethylthiazol-2-yl)-2,5-diphenyltetrazolium bromide assay

The 3-(4,5-dimethylthiazol-2-yl)-2,5-diphenyltetrazolium bromide (MTT) assay was performed according to Mosmann [36]. Briefly, cells were seeded in a 96-well dish for 24 h, and treated with different concentrations of compound (1-50 µM) at 37° C for 24 h. Afterwards, the medium was changed and the cells were incubated with 0.5 mg/mL MTT under normal culture conditions for 3 h. Cell viability was marked by the conversion of the tetrazolium salt MTT to a colored formazan by mitochondrial dehydrogenases. Color development was measured spectrophotometrically with a microplate reader (model 7530, Cambridge Technology, USA) at 570 nm after cell lysis in DMSO (100 µL per well). Cell viability was plotted as the percentage of the control value.

3. Results and Discussion

3.1. Structural results

The H_2L ligand crystallizes as E isomer in the tautomeric amido form (I) (*Scheme 3*), where the hydrazides fragment adopts the keto-amine arrangement [23]. The C8=N1, C9=O2 and the C9-N2 bond lengths are in close agreement with the formally double and single bond character [37] and also with the reported values for some hydrazones in the amido tautomeric form (I) [38-41].

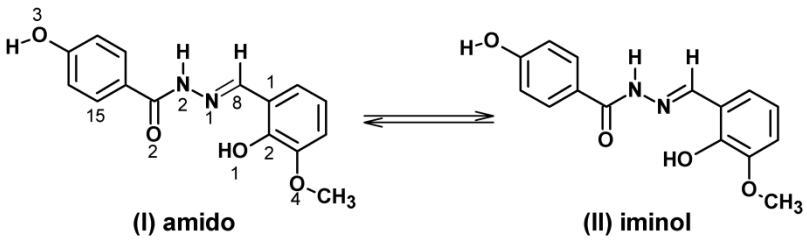

Scheme 3. Schematic representation of the amido-iminol tautomeric equilibrium of H_2L.

The solid state structure of the copper compound, $[Cu(HL)(OH_2)_2](NO_3)$, was determined by X-ray diffraction methods. An ORTEP plot with the atom numbering scheme [42] is shown in Figure 1. In Table 2, some selected experimental geometric parameters of complex (1) are listed together with those reported for the H_2L ligand [23]. Calculated geometric parameters are also included to be forward compared (see below).

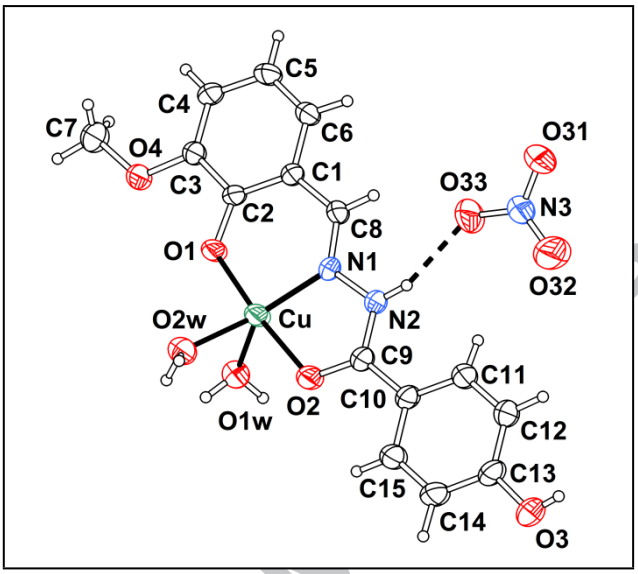

Figure 1. View of $[Cu(HL)(OH_2)_2](NO_3)$ showing the labelling of the non-H atoms and their displacement ellipsoids at the 50% probability level. Metal-ligand bonds are indicated by solid lines.

The structural analysis of the complex reveals that the Cu(II) ion is in a distorted square pyramidal environment, coordinated at the pyramid basis to a nearly planar HL^- monoanion [*rms* deviation of non-H atoms from the least-squares plane of 0.034 Å], tridentate chelator through the phenolate oxygen atom [d(Cu-O1) = 1.899(3) Å], the azomethine nitrogen atom [d(Cu-N1) = 1.919(3) Å] and the carbonyl O-atom [d(Cu-O2) = 1.971(3) Å]. The metal is placed onto the coordination plane [at 0.043(2) Å] of the distorted square basis that is completed with an oxygen atom of one water molecule [d(Cu-O2w) = 2.031(3) Å] whereas the pyramid apex is occupied by the oxygen atom of another water molecule. Similarly to that found with other copper square pyramidal compounds axial elongation is structurally evident for complex (1). [40, 43, 44] The axial Cu-O1w bond distance of 2.307(3) Å is longer than the equatorials ones, which have relatively short bond distances, as can be seen in table 2. The Z-out distortion observed can be interpreted in terms of second order Jahn-Teller effect which arises from non-degenerate states that are close in energy [44, 45]. Due to the coordination of HL^- with the copper ion, one five-member (CuO2C9N2N1) and other six-member (CuO1C2C1C8N1) chelate ring that share the

Cu- N1 bond, are formed.

The structure and metrics of the $[Cu(HL)(OH_2)_2]^+$ cation complex are closely related to the one reported for $[Cu(HL)(CH_3OH)_2]^+$ in $[Cu(HL)(CH_3OH)_2](NO_3).CH_3OH$ crystal, where two methanol molecules are coordinated to the metal ion instead of the water molecules [40].

Crystallographic data show that bond distances and angles within the HL^- ligand are also in general agreement with the corresponding values reported for H_2L [23]. Both phenyl rings show the delocalized resonant-bond structure with C-C bond lengths from 1.370(5) to 1.391(5) Å for the hydrazide fragment and from 1.360(5)-1.408(5) Å for the aldehyde fragment of the N-acyl hydrazone. Moreover, the C9=O2 and C9-N2 bond lengths of 1.260(4) and 1.336(5) are also in close agreement with those found in several hydrazones that coordinate with metal ions as HL^-, in the amido tautomeric form (I) [38-41]. It must be noted that for hydrazones that coordinate in the tautomeric form (II) (Scheme 3) the expected bond lengths are about 1.29-1.31 Å for C-O(H) and 1.28-1.32 A° for C=N [38].

Table 2. Selected experimental and calculated geometric parameters for the three conformers I, II and III of the hydrazone ligand, H_2L, (see below) and for complex (1). Bond distances are in Angstroms [Å]. Bond angles are in degrees [°]. See Figure 1 for labels.

	H_2L				Complex (1)	
Bond distances	**Exp.[a]**	**I**	**II**	**III**	**Exp.**	**Calc.**
C2-O1	1.352 (6)	1.343	1.343	1.339	1.320 (4)	1.306
C1-C2	1.407 (7)	1.408	1.408	1.409	1.408 (5)	1.428
C1-C8	1.440 (7)	1.453	1.454	1.449	1.431 (5)	1.422
C8-N1	1.279 (6)	1.291	1.291	1.283	1.292 (5)	1.297
N1-N2	1.385 (6)	1.368	1.368	1.354	1.378 (4)	1.373
C9-N2	1.328 (6)	1.376	1.377	1.385	1.336 (5)	1.356
C9-O2	1.240 (6)	1.221	1.221	1.213	1.260 (4)	1.259
C9-C10	1.480 (7)	1.496	1.496	1.494	1.459 (5)	1.459
Cu-N1	-	-	-	-	1.919 (3)	1.939
Cu-O1	-	-	-	-	1.899 (3)	1.886
Cu-O2	-	-	-	-	1.971 (3)	1.990
Cu-O1w	-	-	-	-	2.307 (3)	2.423
Cu-O2w	-	-	-	-	2.031 (3)	2.060
Bond angles	**Exp.**	**I**	**II**	**III**	**Exp.**	**Calc.**
O1-Cu-N1	-	-	-	-	92.9 (1)	93.1
O1-Cu-O2	-	-	-	-	174.0 (1)	174.4

N1-Cu-O2	-	-	-	-	81.2 (1)	81.2
O1-Cu-O2w	-	-	-	-	93.1 (1)	87.2
N1-Cu-O2w	-	-	-	-	149.1 (2)	161.7
O2-Cu-O2w	-	-	-	-	92.6 (1)	98.1
O1-Cu-O1w	-	-	-	-	90.0 (1)	88.5
N1-Cu-O1w	-	-	-	-	123.6 (1)	117.5
O2-Cu-O1w	-	-	-	-	92.1 (1)	94.0
O2w-Cu-O1w	-	-	-	-	86.7 (1)	80.8

a) Experimental data extracted from Ref [23]. Atom labels are consistent with those of Figure 1, for comparison. A complete list of experimental geometrical parameters of complex (1) is available in Tables S1-S3 (ESI).

As expected, the major changes occur at the groups involved in the binding to the metal. In fact, upon deprotonation and coordination to copper, the C2-O1 bond length shortens from d(C-OH) = 1.352(6) Å value reported for H_2L to d(C-O) = 1.320(4) Å observed in the complex (4.6 times the standard error σ). When compared with the H_2L molecule, the imine (H)C8=N1– formally double bond lengthens in 0.013 Å (2σ) upon nitrogen linking to the metal as coordinated carbonyl C9=O2 group (+0.020 Å, 3σ) does.

As shown in Figure 2, neighbouring complexes are arranged in the lattice as centrosymmetric dimers stabilized through bifurcated OwH…O bonds that involve as acceptors the phenolate (O1) and methoxy (O4) oxygen atoms [OwH…O bond distances in the 2.14(3)-2.28(4) Å range]. Neighbouring dimers, in turn, are bridged through NH..NO_3…HO bonds [d(N2H..O(nitrate)) = 2.08(5) Å, ∠(N2-H…O(nitrate)) = 161(5)º; d(O3H..O(nitrate)) = 2.10(5) Å, ∠(O3-H…O(nitrate)) = 150(5)º] giving rise to a ribbon-like polymeric structure that extends along the crystal [121] direction. The ribbon-like motifs are assembled by Ow-H···O(nitrate) bonds [d(Ow1H···O31(nitrate) = 2.06(2) Å, ∠(Ow1-H1A···O31(nitrate)) = 166(5)°], which could be assisted by π···π contacts, established between the six CuN1C8C1C2O1 or five CuN1N2C9O2 member pseudo-rings and the ring of the aldehyde fragment [ring plane distances are less than 3.5 Å], that further stabilize the 3D crystal structure. The H-bonding structure between ribbon-like motifs is depicted in Figure S1 and further detailed in Table S4 (ESI).

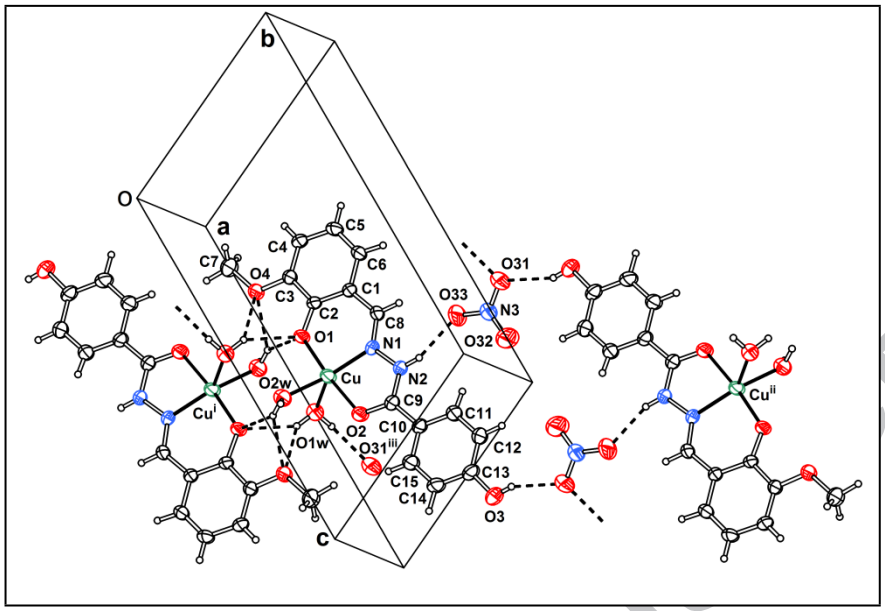

Figure 2. H-bonds network of $[Cu(HL)(OH_2)_2](NO_3)$ complex, in dashed lines, building a ribbon-like structural motif. Metal-ligand bonds are indicated by solid lines. Symmetry operations: (i) -x+1, -y, -z+1; (ii) -x+2, -y+2, -z+2; (iii) x, y-1, z

3.2. Optimized geometries of H_2L and complex (1) and their comparison with experimental data

The conformational searching for the hydrazone ligand, H_2L, led to two very similar structures, **I** and **II**, which are separated by only 0.17 kcal mol^{-1}. The H_2L geometry optimized from the experimental structure, **III**, was found 0.49 kcal mol^{-1} above conformer **I**. The three conformers are shown in Figure S2 of ESI. Selected calculated geometric parameters of the three stable conformers found for H_2L and of the complex (1) were compared with experimental data as a validation for the computational methodology used throughout. Lattice effects are completely ignored as calculations were performed in the gas phase.

As can be seen in Table 2, bond distances are well described in general for H_2L. The larger discrepancies are observed around C9, that is, the C9-N2 and C9-O2 bonds and, in a lesser extent the C8-C1 bond, exhibit errors in the range 0.02 - 0.06 Å (for atom numbering see Figure 1). Errors of about 0.02- 0.03 Å are observed for N1-N2. On the other hand, calculated and experimental bond distances of the complex (1) are in very good agreement, with errors of about 0.02 Å. The larger error is observed for the Cu-O1w bond distance, for which the calculated value becomes 0.116 Å larger than the experimental one. It is argued that lattice effects, which are absent in present calculations, could play an important role in stabilizing such a large Cu-O1w

bond. Interestingly, the Cu-O2w bond, which is considerably shorter than the Cu-O1w one, is well reproduced by present calculations with an error of about 0.03 Å.

There is a good agreement between experimental and calculated bond angles in the case of H_2L (Table S5). As expected, the larger errors are observed for conformers **I** and **II** around the C9-N2-N1=C8 moiety, which was used to generate starting geometries for the conformational searching. Conformer **III**, on the other hand, shows the better agreement with the experimental structure.

Minor changes are observed in the ligand bond angles when the complex is formed. The agreement between observed and calculated values is very good (Table S5). Bond angles involving the metal ion and the N1, O1 and O2 atoms are very good described by present calculations, as can be seen in Table 2. The larger errors are observed in those bond angles involving O1w and O2w, that is, oxygen atoms belonging to the water molecules. Those discrepancies could also be attributed to the presence of non-negligible lattice effects.

Calculated torsion angles of conformer **III** are in good agreement with experimental values (Table S5). As calculated gas phase geometry and experimental solid state structure exhibit similar conformations this seems to indicate that the ligand is subject to small lattice effects. The only relevant difference between the experimental structure and the optimized geometry of conformer **III** is the relative orientation of the OCH_3 group, measured as C7-O4-C3-C2, which is found below and above the *o*-HVA ring plane in the experimental and the calculated structures, respectively.

It can be seen from Table 2 and also from Figure S2 that conformers **I** and **II** exhibit very similar structures, differing mainly in the relative orientation of the O3-H group of the 4-HBH ring. The most relevant difference between conformers **I** and **II** and the experimental structure is found in the C8-N1-N2-C9 torsion angle. That torsion angle is very close to 180 degrees both for the experimental structure, and also for conformer **III**, whereas it is close to 0 degrees for conformers **I** and **II**. Those differences could be attributed to the relatively free rotation around the N1-N2 bond that takes place both in the gas phase and in the presence of solvent effects.

The larger discrepancies between experimental and calculated torsion angles are observed for those angles in which the oxygen atoms of the water molecules are involved. The C9-O2-Cu-O2w torsion angle shows the larger error, which is about 20 degrees.

It is also interesting to note that the C11-C10-C1-C2 torsion angle, which indicates the dihedral angle between the two aromatic rings, shows an excellent agreement between experimental and calculated values. That torsion angle is found to be -146.6 degrees from the CIF file of reference 23, whereas it is -153.4 degrees for conformer **III**. On the other hand, the torsion angle shows

values of -23.6 and 26.2 degrees for **I** and **II**, respectively. For complex (1) the agreement is also very good, the experimental and calculated values being -179.2 and -170.6 degrees, respectively.

3.3. EPR spectroscopy

X-band EPR measurements were carried out on a powdered sample of complex (1) in the 0-700 mT region. The EPR spectra recorded at 150 K and 298 K show no relevant changes with temperature (Figure S3 of ESI).

The calculated *g*-values arisen from the best fit to the experimental data are: g_1 = 2.264, g_2 = 2.069 and g_3 = 2.050 (Figure 3). The features are characteristic of Cu(II) ions with $d_{x^2-y^2}$ ground-state, which agrees well with the square pyramidal geometry evidenced by the crystallographic results (Addison's parameter τ = 0.42) [46]. The *G*-value is 4.44 (Equation 1) [47], within the 4.0-4.5 range in good accordance with the absence of noticeable magnetic coupling between the monomeric paramagnetic species in the crystal structure.

$$G = \frac{g_{\parallel} - 2}{g_{\perp} - 2} \qquad \text{Equation 1}$$

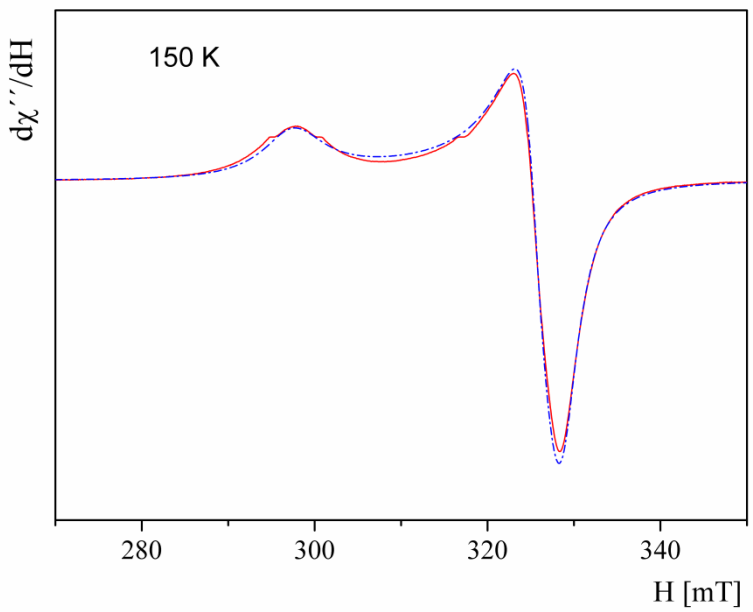

Figura 3. EPR spectrum of complex (1) at 150 K (solid line) together with the best fit (dashed line).

3.4. Vibrational spectroscopy

The solid state vibrational properties of H_2L and complex (1) were analyzed by FTIR and Raman spectroscopies. Comparative FTIR and Raman spectra of each compound are given in Figure S4. For the assigment of the experimental bands of H_2L, its FTIR spectrum was first compared with those of the *o*-HVA and 4-HBH precursors. Some selected experimental and calculated wavenumbers are given in Table 3 (for atom numbering see Figure 1). A complete list of the

experimental and calculated wavenumbers along with the proposed assignment is given in Table S6 (ESI). The proposed assignments, which are briefly discussed below, were done based on literature data [48-50], our previous studies with related compounds [21, 51] and with the support of the wavenumbers calculated with the same level of theory for conformer (III), complex (1) and the precursors.

In the spectrum of H_2L the absence of the bands assigned to the ν(C=O) mode of the aldehyde precursor (*o*-HVA) [51] and those attributed to the different NH_2 vibration modes of 4-HBH clearly confirms the formation of the hydrazone [49].

According to calculation, the very strong absorption at 1646 cm^{-1} can be ascribed to the mixed normal mode involving the ν(C=O2) of 4-HBH and the δ(CN2-H) in-plane deformation. A new strong IR band at 1608 cm^{-1} (Ra: 1609 cm^{-1}) is assigned to the expected stretching vibration of the azomethine group, ν(C=N1), which is coupled with the carbon-carbon stretching of the *o*-HVA ring. In the complex, this IR band shift slightly to lower frequencies (IR: 1603 cm^{-1}) indicating, in accordance with crystallographic data, a decrease in the C=N1 double bond character (see Table 2) due to the coordination of the azomethine nitrogen to the copper ion. Quantum chemical calculations predict that the ν(C=N1) mode is coupled with the ν(C=O2) and with the carbon-carbon stretching of the *o*-HVA ring in complex (1). An upward shift by 32 cm^{-1} of the band at 1186 cm^{-1}, assigned to ν(N-N) mode of the hydrazone, also supports the involvement of N1 in the coordination. Furthermore, the presence of different absorption bands due to the normal vibration modes of the N2H group agree with the coordination of the ligand in the amido tautomeric form (I). The strong absorption at 1384 cm^{-1} undoubtedly indicates the presence of nitrate in ionic form [50, 52].

In the higher region of the *o*-HVA precursor IR spectrum, a weak absorption band at 3014 cm^{-1} was assigned to the phenolic O-H stretching vibration [51]. The intensity and absorption position of the band was attributed to the so-called chelation structure originated by intramolecular hydrogen interaction between the OH and the neighboring conjugate C=O group of the aldehyde [49]. In the H_2L free ligand the formation of a six-member pseudo-ring (N1C8C1C2O1) by a strong O1H···N1 intra-molecular interaction apparently affects in a similar way the intensity and frequency of the OH stretching band (calculated at 3380 cm^{-1}), which could not be detected in the H_2L spectrum. Thus, the involvement of the phenolate oxygen (O1) in the coordination is corroborated by the absence of the in-plane and out-of-plane deformation modes of the O1-H phenol group, which appears in the IR spectrum of the ligand at 1368 cm^{-1} and at 837 cm^{-1}, respectively. It is interesting to mention that the relatively high frequency of the γ(O1H) (IR:837 cm^{-1}, calculated 753 cm^{-1}) is in accordance with the predicted correlation between the strength of

the hydrogen interaction and the expected frequency shifting of the ν(OH) and γ(OH) modes in related compounds [53,54].

In the IR spectrum of the ligand two bands in the 3400-3300 cm^{-1} region are associated with the asymmetric and symmetric OH stretching vibrations of lattice water, which are not considered in the calculations. For the complex, the overlapping of several absorption bands due to the stretching modes of the coordinated water molecules, the ν(O3-H) of the hydrazine fragment, and the ν(N2-H) functional group, give rise to a broad band in the 3400- 3100 cm^{-1}. Many weak bands in the 2850-3100 cm^{-1} spectral region of both compounds correspond to the aromatic and methoxyl CH stretching modes. The corresponding absorptions due to CH in-plane and out-of-plane deformations modes of both rings are also observed in the expected regions [49-51].

Calculation also predict that absorptions at 630 cm^{-1} and 550 cm^{-1} correspond to the rocking and wagging frequencies of the coordinated H_2O(2w) molecule, respectively. It is worth to mention that these modes are predicted at wavenumbers lower than 400 cm^{-1} for the H_2O(1w) molecule. The corresponding bending modes, δ(H_2O), of both molecules are superimposed with the absorptions found in the 1560-1520 cm^{-1} region.

Moreover, in the spectra of complex (1) some absorption bands can be related with vibrations of the pseudo-ring, (O1CCCN1) and (N1NCO2), originated by the coordination. The new band of medium intensity at 1438 cm^{-1} (Ra: 1438 cm^{-1}) is assigned, with the aid of the calculation, to the stretching vibration of the (O1CCCN1) pseudo-ring, whereas the in-plane deformation modes of both rings are calculated at frequencies below 910 cm^{-1}. Besides, weak bands at 577, 506 and 430 cm^{-1} that are not present in the spectra of the free ligand are assigned to ν_s(N1-Cu-O1), ν(Cu-N1) and ν(Cu-O2) modes, respectively. The calculated harmonic vibration frequencies indicate that these modes are coupled with other characteristic vibrations, as can be observed in Table 3.

Table 3. Assignment of some characteristic IR and Raman bands of complex (1), the hydrazone ligand H_2L and their precursors, which are included for comparison. Band positions are in cm^{-1}.

OHVA[a]	4-HBH			H_2L				Complex (1)			
IR	IR	Calc[b]	Assignment	IR	Ra	Calc	Assignment	IR	Ra	Calc	Assignment
1645 vs											$\nu C{=}O^{OHVA}$
	1621 vs	1724	$\nu C{=}O2 + \delta N2H + \delta NH_2$	1646 vs		1746	$\nu C{=}O2 + \delta N2H$				
				1608 s	1609 vs	1669	$\nu C{=}N1 + \nu_R^{OHVA}$	1603 s	1614 s	1653	$\nu C{=}N1 + \nu C{=}O2 + \nu_R^{OHVA}$
1591 sh											$[\nu_R + \delta OH]^{OHVA}$
				1586 w	1592 m	1650	$[\nu_R + \delta OH]^{OHVA}$ + ν_{as} C-C=N1	1561 m	1571 m	1638	$\nu_R^{OHVA} + \nu_{as}$ C-C=N1 + $\delta H_2O^{coord\ 2}$
	1538 m	1625	$[\nu_R + \delta OH]^{HBH}$	1542 sh		1623	$[\nu_R + \delta OH]^{HBH}$	1543 m	1544 m	1622	$[\nu_R + \delta OH]^{HBH} + \delta H_2O^{coord\ 1}$
	1468m-s	1492	$\nu C9N2 + \delta CN2H + \nu_R^{HBH}$	1466 m	1466 sh	1541	$\nu C9N2 + \delta CN2H + \nu_R^{HBH}$	1464 w	1466 sh	1540	$\delta CN2H + \nu C9O2 + \nu_R^{HBH}$
								1438 m	1438 m-s	1437	ν_{QR} [O1C2C1C8N1]
1388 s				1368 m-s	1377 vw	1433	$[\delta OH + \nu_R]^{OHVA}$				
								1384 s,b	1389 vw		$\nu_{as}(NO_3^-)$
	1328 s	1304	$\nu C10C9 + \delta CN2H$	1322 sh	1328 sh	1255	$\nu C10C9 + \delta CN2H$	1322 m, b	1326 m	1301	ν_{as} (C10C9N2) + δCN2H
1327 s				1311m	1314 vs	1307	$\nu C2\text{-}O1(H) + \delta CH^{OHVA}$	1312 sh	1315 m	1347	$\nu C2\text{-}O1 + [\delta CH]^{OHVA + HBH}$
	1279 vs	1291	$[\nu C\text{-}O3(H) + \delta CH]^{HBH}$	1280 m-s	1282 m	1296	$[\nu C\text{-}O3(H) + \delta CH]^{HBH}$	1289 m	1287 m	1328	$[\nu$ C-O3(H) + $\delta CH]^{HBH}$
	1256 s	1194	$[\delta CH + \delta OH]^{HBH}$	1249 m,b		1198	$[\delta CH + \delta OH]^{HBH}$	1249 m		1208	$[\delta CH + \delta OH]^{HBH}$
	1188 w	1215	$\nu N\text{-}N + \nu C10C9 + \delta CH^{HBH}$	1186 m	1190 w	1170	$\nu N\text{-}N + \nu C10C9 + [\delta CH]^{HBH + OHVA}$	1218 s	1219 vw	1164	$\nu N\text{-}N + \nu C10C9 + [\delta CH]^{HBH + OHVA}$
	1174 m	1186	$[\delta OH + \delta CH]^{HBH}$	1172 w	1165 w	1188	$[\delta OH + \delta CH]^{HBH}$	1175 m		1190	$[\delta OH + \delta CH]^{HBH}$
	899 m	892	$\rho_w NH_2 + \delta(N2C9O2) + \delta_R^{HBH}$	894 m	898 w	908	$\delta(N2C9O2) + \delta_R^{HBH}$	907 w	911vw	921	δ_{QR} (N1N2C9O2) + δ_R^{HBH}
	850 m-s	859	$\gamma CHip^{HBH}$	843 m		868	$\gamma CHip^{HBH}$	848 m		872	$\gamma CHip^{HBH}$
838 m				837 sh	839 vw	753	γOH^{OHVA}				
				730 m-w	739 vw	744	$\delta_R^{OHVA} + \delta(N2N1C8)$	747 m		759	$\delta_R^{OHVA} + \delta(N2N1C8) + \delta_{QR}(O1C2C1C8N1)$
								630 sh		635	$\rho_r^{H2O\ coord.2}$
								577 vw	581 vw	581	ν_s (N1-Cu-O1) + $\delta(C3OCH_3)$
								550 vw	550 vw	554	$\rho_w^{H2O\ coord.2}$
								506 vw	499 vw	497	ν(Cu-N1) + δ_{QR}(O1C2C1C8N1)
								430 vw	431 vw	432	ν(Cu-O2)

Calculated frequencies are not scaled. vs: very strong; s: strong; m: medium; w: weak; vw: very weak; sh: shoulder. ν: stretching; δ: in-plane deformation; γ: out-of-plane deformation; ρ_t: twisting; ρ_w: wagging. [a] Assignments for OHVA are extracted from Ref 51. [b] Data obtained in this work with the same level of theory that the employed for H_2L and complex (1).

3.5. Electronic Spectroscopy

The electronic absorption spectra of H_2L and complex (1) were recorded in the 200-800 nm spectral range, both in DMSO and MeOH solutions. The spectra were similar in both solvents, although due to the higher dielectric constant of DMSO a slight red shift of the absorption maxima was observed in solutions of this solvent. The stabilities of H_2L and complex (1) were also determined at room temperature in $2.5x10^{-5}$ M and $1x10^{-3}$ M DMSO and MeOH solutions at various interval times (0-72 h). Results indicate that the compounds are stable in both solutions as the absorbance and the wavelength maxima (λ_{max}) remain constants during the tested interval time.

The following discussion will be centered on spectra obtained in MeOH solutions due to the wider spectral range that can be analyzed (Figure S5). The absorption bands of both compounds were assigned with the aid of TD-DFT calculations. The observed maxima and the calculated transition energies of complex (1) are listed in Table 4. Experimental values of H_2L are also included in the table for comparison (see Tables S7 and S8 of the ESI for detailed information).

Table 4. Electronic spectrum of complex (1) in 1.10^{-5} M methanol solution. Absorption maxima and transition energies are in nm. Extinction coefficients (ε, in $M^{-1}.cm^{-1}$) and oscillator strength of calculated transitions (in atomic units) are in parentheses. The experimental spectra of H_2L and the corresponding assignment are also given.

H_2L	Complex (1)		Assignment
Experimental	**Experimental**	**Calculated**	
217 (22.10^3)	235 (23.10^3)	234 (0.2229)	Intra-ligand transition
301 (29.10^3)	260 (16.10^3)	269 (0.0577)	Charge transfer transition
	306 sh	287 (0.3803)	Charge transfer transition
311 sh	324 (24.10^3)	322 (0.6834)	Intra-ligand transition
	335 (22.10^3)	334 (0.1488)	Intra-ligand transition
336 sh	389 (14.10^3)	422 (0.1245)	Intra-ligand transition
	688 (116)[*a]	574 (0.0005)	d → d
		640 (0.0003)	d → d

[*a] The band was detected using a more concentrated solution (1.10^{-3} M)

As can be seen from the table, the agreement between experimental bands and calculated transition energies is very good. As the conformation adopted by H_2L in the complex is similar to the one of conformer **III** only MO's of that conformer are considered for comparisons with MO's of complex (1). It can be concluded from that comparison that the bands observed at 235, 324 and 389 nm in complex (1) correspond to the bands at 217, 311 and 336 nm in H_2L, respectively. Thus, those

bands can be assigned to intra-ligand transitions. On the other hand, the bands at 260 and 306 nm in complex (1) are assigned to a splitting of the band at 301 nm in H_2L as a consequence of the interaction of MO's located on the ligand and AO's of the metal ion. Those bands can be assigned to charge transfer transitions. The band observed at 335 nm in complex (1) is assigned to a transition from a MO localized at the *o*-HVA fragment to a MO delocalized on the whole H_2L ligand. It is assigned to an intra-ligand transition, although it is not present in the H_2L spectrum. Finally, the band observed at 688 nm is assigned to the characteristic d-d transition of the Cu(II) ion in a distorted square pyramidal environment and it can be described by two transitions at 574 nm and 640 nm, which involve MO's that are mainly localized on the metal ion. A detailed description of the MO's involved in the transitions is provided in the ESI.

3.6. Effect of complex (1) on cell viability in different tumoral cells

To test the effect of chemical complexation on cell viability of tumor cell lines panel, different tumoral cells (MG-63, A549, MCF-7, MDA-MB-231 and Jurkat cells) were exposed to the H_2L ligand, Cu(II) ion and complex (1) during 24 h, at 37°C. The results obtained from these assays indicate that the complex (1) diminished the cell viability from a concentration of 5 µM ($p < 0.01$) and caused an inhibitory effect on MG-63, MCF-7, MDA-MB-231 in the range of 5 to 10 µM, whereas it displayed antiproliferative effect on A549 and Jurkat cells in the range of 10 to 25 µM, as can be observed in Figure 4.

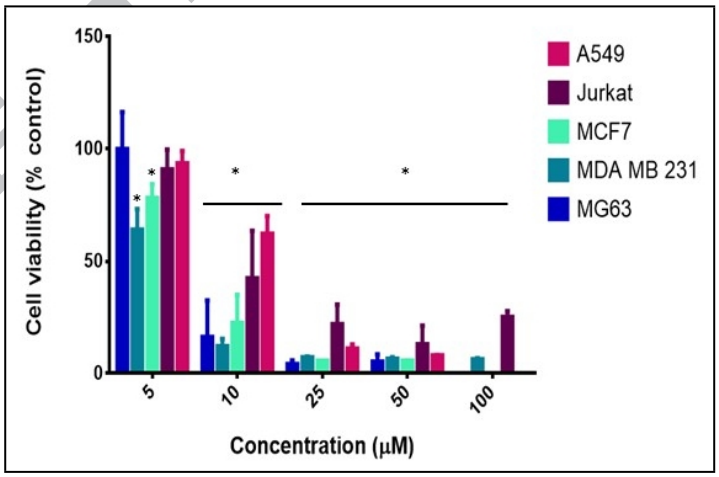

Figure 4. Effects of complex (1) on MG-63, A549, MCF-7, MDA-MB-231 and Jurkat cell viabilty. Cells were incubated in serum-free Dulbecco's modified Eagle's medium (DMEM) alone (control) or with different concentrations of complex (1), at 37 °C, for 24 h. The results are expressed as the percentage of the basal level and represent the mean ± the standard error of the mean (SEM) (n = 18). Asterisk: significant difference in comparison with the basal level *($p < 0.01$).

To determine the antitumoral effectiveness of complex (1), its cytotoxic effects are compared with those of the reference metallodrug cisplatin (CDDP), on the tumor panel cell lines tested. As it can be seen in Table 5, which shows the IC_{50} values obtained for complex (1) and the corresponding ones for CDDP, the copper complex is significantly more cytotoxic than cisplatin on all tested cells. It is also clear from the table that the antitumor effectiveness of the complex on lung, bone, breast, cancer and leukemia cells increases according to the following order of potency: A549 < Jurkat < MG-63 < MCF-7 < MDA-MB-231.

Table 5. IC_{50} values of complex (1) on all the panel cell tested after 24 h of incubation and the corresponding ones for CDDP.

Cell line	IC_{50} (μM) ± SD	
	Complex (1)	CDDP
Jurkat (leukemia)	10.6 ± 0.3	10.8 ± 1.2[(a)]
A549 (lung)	12 ± 1.2	114 ± 9.1[(a)]
MG-63 (bone)	8.8 ± 0.3	39 ± 1.8 [(b)]
MCF-7 (breast)	7.4 ± 1.1	43 ± 3.0 [(b)]
MDA-MB.231 (breast)	5.8 ± 0.4	131 ±18[(a))]

[(a)] Data extracted from reference 55, [b)] This work.

Furthermore, the assays carried out with H_2L and the Cu(II) ion show that both species cause an inhibitory effect in all cell lines panel tested only at high concentration (data not shown). The obtained IC_{50} values are greater than 100 μM indicating that their cytotoxic activity is much lower than that of the complex. Altogether, these results would suggest that the complexation plays an important role in modulating the antitumor activity of the complex which should keep unaltered its coordination sphere at least until it enters in the cells.

In addition, it is interesting to note that several copper complexes with IC_{50} values in the low micromolar to submicromolar range (lower than 10 μM) has been recognized as potent cytotoxic agents against different human cancer cell lines [56]. In accordance with the foregoing and taking into account that complex (1) shows IC_{50} values in the range from 5.8 μM to 12 μM, it could be considered a promising non-platinum anticancer agent with remarkable cytotoxic effectiveness. Probably, as other active copper complexes, it follows a mechanism of action and bio-distribution different from those known for platinum-based chemotherapeutics [13,14]. Nonetheless, to provide insight into its possible mechanism of action and bio-distribution on different human cancer cells, further studies are necessary.

Conclusions

A new copper complex containing the N-acylhydrazone obtained by condensation reaction of 4-hydroxy-benzohydrazide with 2-hydroxy-3-meyhoxybenzaldehyde was synthesized and characterized in the solid state and in solution. The coordination polyhedron consists of a CuO_4N distorted square pyramid, where the hydrazone coordinates to the copper ion in the amido tautomeric form through its O,N,O donor atoms. The other two coordination sites are occupied by the oxygen atoms of two water molecules with the axial bond distance longer than the equatorial one. EPR measurements are consistent with a $d_{x^2-y^2}$ ground state, which correlates well with the distorted square pyramid geometry determined by XRD methods. Geometrical parameters and calculated spectroscopic features also show a very good agreement with experimental data.

The complex inhibits the viability of five human cancer cells lines in a dose dependent manner with a greater potency than the observed for the free ligand and the Cu(II) ion. The anticancer activity of the complex against the panel cell tested is higher than those reported for the reference metallodrug cisplatin. These findings show the significant effect of the chelation on the bioactivity of the complex and suggest that it can be considered a promising candidate for further mechanistic studies as well as for other interesting biological assays.

Acknowledgments. This work was supported by CONICET (PIP 11220130100651CO and PIP 0034), UNLP (111/X673) and ANPCyT (PICT 2014-2223) of Argentina. Consejería de Educación CyL and FFEDER BU076U16, BU022G18 and Ministerio de Economía y Competitividad CTQ2016-75023-C2-1-P and CTQ2015-70371-REDTMetDrugs Network (Spain). I.E.L, G.A.E, O.E.P, R.P-D, A.G-B and B.P-C are members of the Researcher Career of CONICET. J.G-T is member of the Department of Chemistry (University of Burgos, Spain). YB-L, JDP and L.M.B are Doctoral Fellows of CONICET. The authors thank Dr. David Ibáñez Martinez (Department of Chemistry, University of Burgos, Spain) for Raman spectra.

Supplementary Information Available:

Crystallographic structural data has been deposited at the Cambridge Crystallographic Data Centre (CCDC). Enquiries for data can be direct to: Cambridge Crystallographic Data Centre, 12 Union Road, Cambridge, UK, CB2 1EZ or (e-mail) deposit@ccdc.cam.ac.uk or (fax) +44 (0) 1223 336033. Any request to the Cambridge Crystallographic Data Centre for this material should quote the full literature citation and the reference numbers CCDC 1559384.

Supplementary data can be found in the online version of this article (Figures S1-S7, Tables S1-S8) A detailed description of the MO's involved in the electronic transitions of both compounds is also provided.

References

[1] S. Rollas, Ş.G. Küçükgüzel, "Biological Activities of Hydrazone Derivatives", Molecules 12 (2007) 1910-1939.

[2] P. Kumar, B. Narasimhan, "Hydrazides/Hydrazones as Antimicrobial and Anticancer Agents in the New Millennium", Mini-Rev. Med. Chem. 13 (2013) 971-987.

[3] Ł. Popiołek, "Hydrazide - hydrazones as potential antimicrobial agents: overview of the literature since 2010", Med. Chem. Res. 26 (2017) 287-301.

[4] V. Vrdoljak, G. Pavlović, N. Mal tar-Strmećkic, M. Cindrić, "Copper(II) hydrazone complexes with different nuclearities and geometries: synthetic methods and ligand substituent effects", New J. Chem. 40 (2016) 9263-9274.

[5] X. Su, I. Aprahamiam, "Hydrazone-based switches, metallo-assemblies and sensors", Chem. Soc. Rev. 43 (2014) 1963-1981.

[6] D.J van Dijken, P. Kovaříček, S.P. Ihrig, S. Hecht, "Acylhydrazones as widely tunable photoswitches, J. Am. Chem. Soc. 137 (2015)14982-14991.

[7] R.R. Singh, P. Jam, R.P. Singh, "Hydrazones as analytical reagents: a review", Talanta 9 (1982) 77-84.

[8] R. Lazny, A. Nodzewska, "*N*,*N*-dialkylhydrazones in organic synthesis. From simple *N*,*N*-dimethylhydrazones to supported chiral auxiliaries", Chem. Rev. 110 (2010) 1386-1434.

[9] M.V. Angelusiu, S-F. Barbuceanu, C. Draghici, G.L. Almajan, "New Cu(II), Co(II), Ni(II) complexes with aroyl-hydrazone based ligand. Synthesis, spectroscopic characterization and in vitro antibacterial evaluation", Eur. J. Med. Chem. 45 (2010) 2055-2062.

[10] M.M.E. Shakdofa, M.H. Shtaiwi, N Morsy, T.M.A. Abdel-rassel, "Metal complexes of hydrazones and their biological, analytical and catalytic applications: A review", Main Group Chemistry 13 (2014) 187-218.

[11] M.C Linder, M. Hazegh-Azam, "Copper biochemistry and molecular biology", Am. J. Clin. Nutr. 63 (1996) 797S–811S.

[12] H. Tapiero, D.M. Townsend, K.D. Tew, "Trace elements in human physiology and pathology. Copper", Biomed. Pharmacother. 57 (2003) 386-398.

[13] T. Wang, Z. Guo, Copper in medicine: homeostasis, chelation therapy and antitumor drug design. Curr. Med. Chem. 13 (2006) 525-537 and references therein.

[14] C. Marzano, M. Pellei, F. Tisato, C. Santini. "Copper Complexes as Anticancer Agents", Anti-Cancer Agents Med. Chem., 9 (2009) 185-211, and references therein.

[15] K. Hu, G. Zhou, Z. Zhang, F. Li, J. Li, F. Liang, "Two hydrazone Copper (II) complexes: Synthesis, crystal structure, cytotoxicity and action mechanism", RSC Adv. 6 (2016) 36077-36084.

[16] D.S. Raja, N.S.P. Bhuvanesh, K. Natarajan, "Structure–activity relationship study of copper(II) complexes with 2-oxo-1,2-dihydroquinoline-3-carbaldehyde (4′-methylbenzoyl) hydrazone: synthesis, structures, DNA and protein interaction studies, antioxidative and cytotoxic activity", J. Biol. Inorg. Chem. 17 (2012) 223-237.

[17] M. Alagesan, N.S.P. Bhuvaneshb, N. Dharmaraj, "Potentially cytotoxic new copper(II) hydrazone complexes: synthesis, crystal structure and biological properties", Dalton Trans. 42, (2013) 7210-7223.

[18] Y.P Singh, R.N. Patel, Y. Singh, R.J. Butcher, P.K. Vishakarma, R.K. Bhubon Singh, "Structure and antioxidant superoxide dismutase activity of copper(II) hydrazone complexes", Polyhedron 122 (2017) 1-15.

[19] V.P. Singh, P. Gupta, "Synthesis, physico-chemical characterization and antimicrobial activity of cobalt(II), nickel(II), copper(II), zinc(II) and cadmium(II) complexes with some acyldihydrazones", J. Enz. Inhib. Med. Chem. 23 (2008) 797-805.

[20] J. Patole, U. Sandbhor, S. Padhye, D.N. Deobagkar, C.E. Anson, A. Powell, "Structural chemistry and in vitro antitubercular activity of acetylpyridine benzoyl hydrazone and its Copper Complex against Mycobacterium smegmatis", Bioorg. Med. Chem. Lett. 13 (2003) 51-55.

[21] A.C. González-Baró, R. Pis-Diez, B.S. Parajón-Costa, N.A. Rey, "Spectroscopic and theoretical study of the o-vanillin hydrazone of the mycobactericidal drug isoniazid", J. Mol. Struct. 1007 (2012) 95-101.

[22] A.C. González-Baró, V. Ferraresi-Curotto, R. Pis-Diez, B.S. Parajón Costa, J.A.L.C. Resende, F.C.S. de Paula, E.C. Pereira-Maia, N.A. Rey. "A novel oxidovanadium (V) compound with an isonicotinohydrazide ligand. A combined experimental and theoretical study and cytotoxity against K562 cells", Polyhedron 135 (2017) 303-310.

[23] J-F Lu, "4-Hydroxy-*N*′-(2-hydroxy-3-methoxybenzylidene)benzohydrazide monohydrate", Acta Cryst. E64, (2008), o2032.

[24] CrysAlisPro, Oxford Diffraction Ltd., version 1.171.33.48 (release 15-09-2009 CrysAlis171.NET).

[25] G. M. Sheldrick, "A short history of *SHELX*", Acta Crystallogr. A64, (2008) 112-122.

[26] WINEPR SimFonia v1.25, Bruker Analytische Messtecnik GmßH, 1996.

[27] Kaleidagraph v3.5 Synergy Software, 2000.

[28] D. Becke, "Density-functional thermochemistry. III. The role of exact exchange", J. Chem. Phys. 98 (1993) 5648-5652.

[29] C. Lee, W. Yang, R. G. Parr, "Development of the Colle-Salvetti correlation-energy formula into a functional of the electron density", Phys. Rev. B. 37 (1988) 785-789.

[30] F. Neese, The ORCA program system, Wiley Interdiscip. Rev Comput Mol Sci. 2 (2012) 73-78.

[31] F. Weigend, R. Ahlrichs, "Balanced basis sets of split valence, triple zeta valence and quadruple zeta valence quality for H to Rn: Design and assessment of accuracy", Phys. Chem. Chem. Phys. 7 (2005) 3297-3305.

[32] C. Adamo, V. Barone, "Toward reliable density functional methods without adjustable parameters: The PBE0 model", J. Chem. Phys. 110 (1999) 6158-6170.

[33] T.H. Dunning, Jr., "Gaussian basis sets for use in correlated molecular calculations. I. The atoms boron through neon and hydrogen", J. Chem. Phys. 90 (1989) 1007.

[34] N.B. Balabanov, K. A. Peterson, "Systematically convergent basis sets for transition metals. I. All-electron correlation consistent basis sets for the 3d elements Sc–Zn". J. Chem. Phys. 123 (2005) 064107.

[35] A. Klamt, G. Schüürmann, "COSMO: a new approach to dielectric screening in solvents with explicit expressions for the screening energy and its gradient", J. Chem. Soc., Perkin Trans. 2 (1993) 799-805.

[36] T.T. Mosmann, "Rapid colorimetric assay for cellular growth and survival: application to proliferation and cytotoxicity assays", J. Immunol. Methods 65 (1983) 55.

[37] F.H. Allen, A. Kennard, D.G. Watson, L. Brammer, A.G. Orpen, R. Taylor, "Tables of Bond Lengths determined by X-Ray and Neutron Diffraction. Part I. Bond Lengths in Organic Compounds", J. Chem. Soc. Perkin Trans. 2 (1987) S1-S19.

[38] H. Hosseini-Monfared, H. Falakian, R. Bikas, P. Mayer, "Intramolecular hydrogen bond effect on keto-enolization of aroylhydrazone in copper(II) complexes", Inorg. Chim. Acta 394 (2013) 526-534

[39] R. Bikas, V. Kuncser, J. Sanchiz, G. Schinteie, M. Siczek, H. Hosseini-Monfared, T. Lis, "Structure and magnetic behavior of unpredictable EE-azide bridged tetranuclear Mn(II) complex with ONO-donor hydrazone ligand and its transformation to dinuclear Mn(III) complex", Polyhedron 147 (2018) 142–151

[40] H. Hosseini-Monfared, E. Pousaneh, S. Sadighian, S.W. Ng, E.R.T. Tiekink, "Syntheses, structures, and catalytic activity of Copper(II)-aroylhydrazone complexes", Z. Anorg. Allg. Chem. 639(2) (2013) 435-442.

[41] Xu, B. Tang, L. Gu, P. Zhou, H. Li, "Open coordination sites-induced structural diversity of a new series of Cu(II) complexes with tridentate aroylhydrazone Schiff base, J. Mol. Struct. 1120 (2016) 205-214.

[42] L. J. Farrugia, ORTEP-3 for windows - a version of ORTEP-III with a graphical user interface (GUI), J. Appl. Crystallogr. 30 (1997) 565-566.

[43] R.Bikas, F. Ajormal, M. Emami, N. Noshiranzadeh, A. Kozakiewicz, "Catalytic oxidation of benzyl alcohols by new Cu(II) complexes of 1,3-oxazolidine based ligand obtained from a solvent free reaction", Inorg. Chim. Acta 478 (2018) 77-87

[44] S.Roy, P.Mitra, A.K. Patra, "Cu(II) complexes with square pyramidal $(N_2S)CuCl_2$ chromophore: Jahn–Teller distortion and subsequent effect on spectral and structural properties, Inorg. Chim. Acta 370 (2011) 247-253.

[45] R.G. Pearson, "Concerning Jahn-Teller Effects (first-order, pseudo, and second-order Jahn-Teller effects/symmetry rules) Proc. Nat. Acad. Sci. USA 72 (6) 6, 1975, 2104-2106, June 1975

[46] A. W. Addison, T.N. Rao,J. Reedijk, J. van Rijn, G.C.J. Verschoor, "Synthesis, structure, and spectroscopic properties of copper(II) compounds containing nitrogen-sulphur donor ligands; the crystal and molecular structure of aqua[l,7-bis(N-methylbenzimidazol-2'-yl)-2,6-dithiaheptane]copper(ii) perchlorate", Chem. Soc. Dalton Trans. (1984) 1349–1356.

[47] B.J. Hathaway, D.E. Billing, "The electronic properties and stereochemistry of mononuclear complexes of the copper ion", Coord. Chem. Rev. 5 (1970)143-207

[48] V. Arjunan, A. Jayaprakash, K. Carthigayan, S. Periandy, S. Mohan, "Conformational, structural, vibrational and quantum chemical analysis on 4-aminobenzohydrazide and 4-hydroxybenzohydrazide - A comparative study", Spectrochim. Acta Part A 108 (2013) 100-114.

[49] D. Lin-Vien, N.B. Colthup, W.G. Fately, J.G. Grasselli in: "Infrared and Raman Characteristic Frequencies of Organic Molecules", Academic Press, Boston, 1999.

[50] K. Nakamoto, in: "Infrared and Raman Spectra of Inorganic and Coordination Compounds", Sixth ed., J. Wiley & Sons, Inc., Hoboken, New Jersey (2009).

[51] A.C. González-Baró, R. Pis-Diez, C.A. Franca, M.H. Torre, B.S. Parajón-Costa, "Physicochemical characterization of Cu(II) complexes with SOD-like activity, theoretical studies and biological assays", Polyhedron, 29 (2010) 959-968.

[52] B.M. Gatehousse, E. Livingston, R.S. Nyholm, "Infrared Spectra of Some Nitrato-co-ordination Complexes", J. Chem. Soc. (1957) 4222-4225.

[53] R.A. Nyquist, "The O-H out-of-plane deformation in intramolecularly hydrogen bonded phenols", Spectrochim. Acta, 19 (1963)1655-1684.

[54] R. Pis-Diez, G.A. Echeverría, O.E. Piro, J.L. Jios, B.S. Parajón-Costa, "A structural, spectroscopic and theoretical study of an o-vanillin Schiff base derivative involved in enol-imine and keto-amine tautomerism". New J. Chem. 40 (2016) 2730-2740.

[55] M. Frik, A. Martínez, B.T. Elie, O. Gonzalo, D. Ramírez de Mingo, M. Sanaú, R. Sánchez-Delgado, T. Sadhukha, S. Prabha, J. W. Ramos, I. Marzo, M. Contel, "In vitro and in vivo evaluation of water-Soluble iminophosphorane ruthenium(II) compounds. A potential chemotherapeutic agent for triple negative breast cancer", J. Med. Chem. 57 (2014) 9995-10012.

[56] C.S. Antini, M. Pellei, V. Gandin, M. Porchia, F. Tisato, C. Marzano, "Advances in Copper Complexes as Anticancer Agents", Chem. Rev. 114, (2014) 815-862, and references therein.